Oxidative Carbonylation of Methanol to Dimethyl Carbonate Over Cu/AC Catalysts Prepared by Microwave Irradiation

J. Ren[*], L.L. Yang, D.L. Wang, Z.F. Qin, Y.L. Pei, J.Y. Lin and Z. Li

Key Laboratory of Coal Science and Technology (Taiyuan University of Technology), Ministry of Education and Shanxi Province, Taiyuan 030024, P.R. China

*Corresponding author: Tel/Fax: +86 351 6018598; E-mail: renjun@tyut.edu.cn

The Cu/AC catalysts were prepared by impregnation of activated carbon with copper nitrate followed by microwave heating in vacuum. They were subsequently tested with the oxidative carbonylation of methanol to dimethyl carbonate. X-ray diffraction, N_2 adsorption, Temperature-programmed reduction, X-ray photoelectron spectroscopy and scanning electron micrographs were used to examine the bulk and surface properties of the carbon-supported copper catalysts. Microwave irradiation causes fast decomposion of copper nitrate and further auto-reduction of copper(II) species to copper(I) oxide and Cu metal induced by the intereaction with the carbon support. The catalytic performance of the Cu/AC catalysts is mainly dependent on the dispersion and grain size of Cu nanoparticles and reaches its optimum for the sample with an irradiation temperature of 350 °C.

Keywords: Dimethyl carbonate, Microwave heating, Cu/AC catalysts, Auto-reduction, Cu Nanoparticles.

INTRODUCTION

Dimethyl carbonate (DMC) has considerable potential as both a chemical intermediate and a fuel additive. It can also be used as a precursor for carbonic acid derivatives and as a methylating agent. Because of its high oxygen content, dimethyl carbonate has been proposed as a replacement for methyl *tert*-butyl ether (MTBE) as a fuel additive[1]. Dimethyl carbonate is currently produced *via* the oxidative carbonylation of methanol on a simple CuCl catalyst in a slurry reactor[2]. Since this process gives rise to severe equipment corrosion and catalyst deactivation, there has been considerable effort directed towards the development of more efficient catalyst systems. High catalytic activity and selectivity can be obtained on homogeneous catalytic systems by properly choosing the supporting ligand[3-6]. Attempts were also made to heterogenize homogenous catalyst systems by immobilizing CuCl or CuCl₂ on polymer supports[7,8] or mesoporous materials[9]. In addition, the development of low-chlorine content or chloride-free catalyst systems for dimethyl carbonate synthesis is a possible new direction[10].

Recent interest has focused on the vapor-phase oxidative carbonylation of methanol over supported copper-based catalysts because this process has been found to be almost free from corrosion[11]. Copper(II) chloride-based catalysts such as CuCl₂, CuCl₂-PdCl₂ or CuCl₂, promoted by acetates or hydroxides suffer from severe deactivation due to the loss of the chloride involved in the reaction[12-15]. There have been attempts to improve the catalyst stability such as immobilization of the active species on functionalized mesoporous silica and replacing chloride by a negatively charged zeolite framework. Yuan *et al*.[16] reported that CuCl₂ supported on amino functionalized MCM-41 and MCM-48 was more active and gave more reliable dimethyl carbonate yield in comparison with those with CuCl₂ supported on non-functionalized mesoporous silicas.

King[17] showed that copper-exchanged Y zeolite catalysts, prepared by a solid-state ion exchange method (SSIE), displayed good productivity and selectivity for dimethyl carbonate synthesis with strongly enhanced stability compared with the usual activated charcoal supported chloride-based catalysts. Various Cu-exchanged zeolites obtained by the SSIE method, such as Cu-MCM-41[18], Cu-X[19], Cu-ZSM-5[20], as well as Cu/β[21] have been extensively investigated as potential candidates for vapor-phase dimethyl carbonate synthesis. Detailed experimental and theoretical investigations on the mechanisms of dimethyl carbonate synthesis on Cu-Y have been reported by Bell *et al*.[22,23]. Richter *et al*.[24,25] recently found that incipient wetness impregnation of zeolite Y with copper(II) nitrate solution and inert activation at 650 °C could lead to chloride-free Cu-zeolite catalysts for the oxidative carbonylation of methanol to dimethyl carbonate in the gas phase at both normal and elevated ambient pressure.

It has been found that chloride is not necessary for the oxidative carbonylation of methanol to dimethyl carbonate over supported copper catalysts. King[17] showed that both Cu(I)Y and Cu_2O/HY catalysts have similar initial activities. However, the Cu_2O/HY catalyst started to deactivate after 1.5 h on stream, which may be attributed to the presence of incomplete exchange sites, which can cause coke formation[26]. Wang *et al.*[27] found that the transformation of CuO and Cu_2O, both present on the CuO-La_2O_3/AC catalyst, complete the catalytic cycle of the oxidative carbonylation of methanol. Li and Wang[28] studied chloride-free activated carbon supported copper catalysts and indicated that the CuO, Cu_2O, or Cu^0 was active for the synthesis of dimethyl carbonate and the catalytic activity increased in the order CuO < Cu_2O < Cu^0. In our previous work, highly dispersed Cu/C catalysts were prepared using $Cu(NO_3)_2$ and starch as primary source materials[29]. Further-more, a detailed study of the mechanism of dimethyl carbonate formation on Cu^0/AC Catalysts was performed using the DFT method and the main pathway of dimethyl carbonate formation is presented. The calculated results provide powerful support for the use of highly active Cu^0/AC catalysts for the synthesis of dimethyl carbonate formation[30].

Microwave heating has attracted much attention in the preparation of catalysts since it causes rapid and even heating, leading to uniform distribution of the active components in the support. In addition, it can alter the activity and selectivity in certain reactions[31-35]. In a previous paper, we prepared highly dispersed CuCl/SiO_2-TiO_2 catalysts through microwave heating and used them for the synthesis of dimethyl carbonate *via* the oxidative carbonylation of methanol in the liquid phase[36]. In the present work, we report a novel Cu/AC catalyst prepared through an auto-reduction method by microwave heating the precursors in a vacuum. This exhibits excellent catalytic performance for the methanol gas-phase oxidative carbonylation of methanol. The influences of microwave treatment temperature on the catalytic performance of the Cu/AC catalysts in the synthesis of dimethyl carbonate have been investigated. The catalysts were characterized by X-ray diff-raction, temperature-programmed reduction, X-ray photo-electron spectroscopy and scanning electron microscopy to establish a fundamental understanding of the relationship between the catalytic performance and the nature of the active sites in the carbon-supported copper catalysts.

EXPERIMENTAL

Catalyst preparation: The activated carbon (AC) used in this work is a commercial product from Xinhua Chemical Plant (Taiyuan, China), which was crushed into particles of 40-60 mesh (0.3-0.45 mm) before use. The activated carbon has a specific surface area of 864 m^2/g, a micro-pore volume of 0.22 mL/g and a mesopore volume of 0.27 mL/g. The Cu/AC catalysts were prepared by the impregnation method. A typical procedure was as follows: 3.2 g of activated carbon was impregnated with a solution of 2.44 g of $Cu(NO_3)_2 \cdot 3H_2O$ dissolved in 5 mL of deionized water at 70 °C for 12 h. The water was removed by heating and drying was carried out at 90 °C for 12 h. The loading of Cu was 16.7 wt. % in the resul-ting catalyst.

The samples were mixed with quartz grain (40-60 mesh) using a weight ratio of 1: 1.5 and then subjected to microwave heating in a microwave experimental setup (Jiequan NJZ4-3, 2.45 GHz, 0-4.2 kW). The heating of the powder mixture was carried out in an alumina crucible with a vaccum pressure of - 0.05 MPa. The sample temperature was ramped to 250 °C, 350 or 450 °C, at a rate of 0.4-0.6 °C/s with output power of 0.05-0.6 kW and then cooled to room temperature. The dried mixtures were sieved through a 0.8 mm screen. The resulting catalysts were stored in a dry box.

Characterization technique and procedures: X-ray diffraction (XRD) data were recorded on a Rigaku D/max 2500 diffractometer using CuK_α radiation (40 kV and 100 mA) over a 2θ range of 10°-80° at a scanning rate of 1°/min. The Brunauer-Emett-Teller (BET) surface area (S_{BET}) and desorption pore volume (V_p) were evaluated using the Barrett-Joyner-Halenda (BJH) method and determined by N_2 physisorption at -196 °C using a SORPTMATIC 1990 system (CE, Italy). Before measure-ment, the sample was degassed at 120 °C until a final pressure below 0.1 Pa was achieved.

Temperature-programmed reduction (TPR) measurements were performed with a Finsore-3010 chemisorption analyzer (Finetec Instruments) equipped with a TCD for monitoring the H_2 consumption from a feed stream containing 10 vol % H_2 in Ar. In these experiments, 50 mg of catalyst was loaded in the reactor. This was purged with pure Ar from room tempe-rature to 200 °C with a heating rate of 10 K min^{-1} then held at this temperature for 1 h. The temperature was then reduced to 50 °C. The reducing mixture was introduced at 20 mL/min and heating was started using a 10 °C/min gradient to 500 °C. The consumption of H_2 was determined using a thermal conduc-tivity cell. Temperature-programmed reduction measurements were carried out from 50 to 500 °C at a heating rate of 10 K min^{-1}.

X-ray photoelectron spectroscopy (XPS) data were collected on an ESCALab220i-XL electron spectrometer (VG, UK) using 300 W Al K_α radiation. The samples were com-pressed into a pellet of 2 mm thickness and then mounted on a sample holder by utilizing double-sided adhesive tape for XPS analysis. The sample holder was then placed into a fast entry air load-lock chamber without exposure to air and evacuated under vacuum (< 10^{-6} Torr) overnight. Finally, the sample holder was transferred to the analysis chamber for XPS study. The base pressure inside the analysis chamber was usually maintained at better than 10^{-10} Torr. The binding energies were referenced to the C1s line at 284.6 eV from adventitious carbon. The curve deconvolution of the obtained XP spectra was performed by using XPS Peak Fitting Program (XPSPEAK41, Chemistry, CUHK).

Scanning electron micrographs (SEM) were obtained with a JEOL-JSM-6701F instrument able to give magnifications of 100,000. An accelerating voltage of 20 kV was used for the analysis. The samples were coated with gold and micrographs of the particles were taken with polaroid camera.

Vapor-phase oxidative carbonylation of methanol: The vapor-phase dimethyl carbonate synthesis by oxidative carbonization of methanol with carbon monoxide and oxygen was investigated using a continuous flow system with a fixed bed reactor. The reactor was a stainless steel tube having an

inner diameter of 10 mm and a length of 40 cm. About 0.25 g (0.3 mL) catalyst, mixed with quartz grains, was packed in the tubular reactor. Methanol was introduced using a syringe pump into the pre-heater, where it was vaporized. The methanol then entered the reactor, together with carbon monoxide and oxygen. An electronic mass flow controller regulated the flow rate of carbon monoxide and oxygen. The reaction products leaving the reactor passed through an ice-water cooling trap and were separated by a gas-liquid separator. The liquid products were then weighed and measured with a flame ionization detector (FID) equipped with a 30 m capillary column of fused silica containing RSL 160 liquid phases for the separation of methanol, dimethyl carbonate, methyl formate (MF), dimethoxy methane (DMM) and dimethyl ether (DME). The uncondensed gas products (O_2, CO_2 and CO) were introduced to the GC through an on-line six-way valve and analyzed by TCD detection with a TDX-01 packed column.

RESULTS AND DISCUSSION

Microwave heating behaviour: The Cu/AC precursors were heated in the microwave oven with a variable output power in order to keep a relative stable heating rate. Fig. 1 shows the variations of the sample temperature as well as power output of the microwave oven with irradiation time. The temperature of the sample rises linearly at first to 70 °C within 3 min, rises quickly to 220 °C then rises linearly at a different heating rate with further increase of the radiation time. Microwave dielectric heating may result in selective heating of catalytic sites with respect to their direct surroundings, leading to "molecular hot spots"[37]. Since the carbon support is a strong microwave absorber[38], hot spot formation at the interface between the copper salts and carbon produces rapid and highly effective dispersion. Further thermal decomposition of copper(II) nitrite at the carbon interface is possible for the Cu/AC precursors. In addition, a lower microwave power output is needed in order to maintain slow and steady heating during microwave radiation.
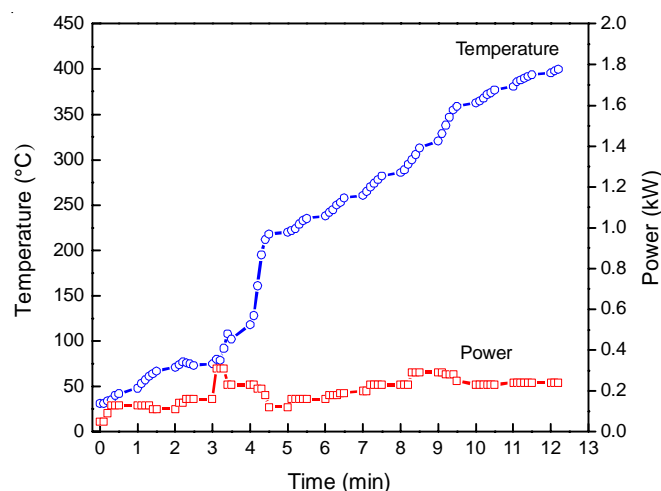
Fig. 1. Microwave heating curve of the Cu/AC precursor

Oxidative carbonylation of methanol: The catalytic activities of Cu/AC catalysts prepared at different temperatures for the gas-phase oxidative carbonylation of methanol are shown in Fig. 2(a) and 2(b). Apart from dimethyl carbonate, the main byproducts detected in the reaction include dimethyl ether (DME), methyl formate (MF) and dimethoxymethane (DMM). The space time yield (STY) of dimethyl carbonate and the conversion of methanol (C_{MeOH}) increase with increasing treatment temperature and show a maximum at 350 °C of 283 mg g^{-1} h^{-1} and 2.56 %, respectively. In addition, there is no obvious difference in the selectivity of dimethyl carbonate.
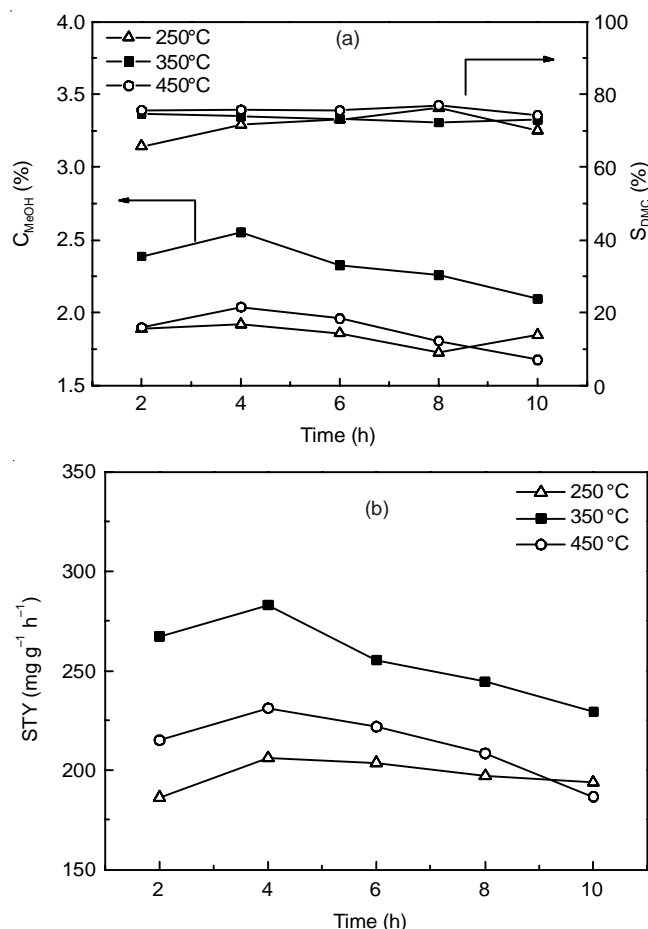
Fig. 2. Catalytic activities of Cu/AC catalysts prepared at different temperatures: (a) MeOH conversion and dimethyl carbonate selectivity and (b) space-time yield of dimethyl carbonate

Characterization of catalysts

XRD: Fig. 3 shows powder XRD patterns of the different Cu/AC catalysts. In all cases, the diffraction peak at 26.5°, corresponding to graphite-C, is observed. Moreover, CuO and Cu_2O were detected in the sample calcined at 250 °C[39]. When the calcination temperature rises to 350 °C, the diffraction peaks of CuO vanish and the diffraction lines of Cu_2O weaken; however, the diffraction lines corresponding to metallic copper then appear[40]. For the sample obtained at 450 °C, the intensity of the diffraction peaks of Cu_2O decrease, but the diffraction lines corresponding to metallic copper become stronger as compared with that obtained at 350 °C.

These observations indicate that the copper precursor was quickly decomposed to CuO under microwave irradiation in a vacuum and was then reduced to Cu_2O and subsequently to metallic Cu with increasing irradiation temperature. It is known that both Cu_2O and Cu^0 are formed as a consequence of the
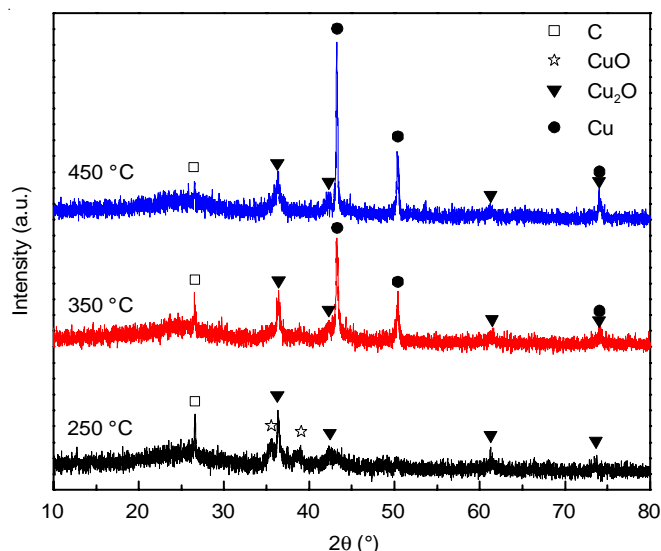
Fig. 3.   Powder XRD patterns of Cu/AC catalysts prepared at different temperatures

reduction of the copper containing compounds by the carbonaceous support[41].

$$2CuO + C \longrightarrow Cu_2O + CO \qquad (1)$$

$$Cu_2O + C \longrightarrow 2Cu + CO \qquad (2)$$
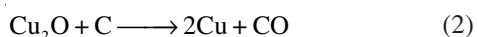
The average crystallite sizes are estimated for Cu_2O and Cu particles by the Scherrer equation. For the sample prepared at 350 °C, the average crystallite sizes for Cu_2O and Cu^0 are 16.8 and 38.3 nm and increase to 23.7 and 46.5 nm, respectively, as the irradiation temperature rises to 450 °C. These results demonstrate that there is clearly a CuO phase formed in the Cu/AC catalyst at an irradiation temperature of 250 °C. With increasing irradiation temperature, the copper species are gradually transformed to Cu_2O and Cu^0 through an autoreduction process by reacting with the carbon support. Furthermore, the grain size of Cu_2O and Cu^0 increase with increasing irradiation temperature. The sample obtained at 350 °C with smaller Cu_2O and Cu^0 particles shows better catalytic activity[42]. This result indicates that the catalytic activity of Cu/AC catalyst is enhanced by the presence of the Cu0 species[28] and smaller Cu^0 particles seem to favor the synthesis of dimethyl carbonate.

N₂-adsorption: A quantitative comparison of the textural structure of the parent carbon supports and the Cu/AC catalysts is given in Table-1. The specific surface area was calculated using the BET model. Total pore volumes were estimated from nitrogen adsorption at a relative pressure of 0.99. The micropore volumes were calculated by the standard *t*-plot method. As can be seen, the S_{BET}, V_p and V_{micro} values are markedly reduced after the dispersion of copper species on the carbon

support. However, the average pore diameters of the Cu/AC catalysts show a slight increase as compared with the carbon support. This is primarily due to pore blockage caused by copper species formed after microwave heating[43].

It can also be seen from Table-1 that the specific surface area and pore volume of the Cu/AC catalysts depend on the temperature of microwave treatment. With increasing treatment temperature from 250 to 350 °C, the values of S_{BET}, V_p and d_p show a marked decrease, indicating that the distribution of the copper species on the carbon support at heating temperatures of 350 °C is relatively uniform[44]. A small decrease in the values of S_{BET}, V_p and d_p occurs for the sample calcined at 450 °C compared to the sample calcined at 350 °C, showing that too high treatment temperature may cause the aggregation of copper species as well as the blockage of pores. This observation is in good agreement with the results obtained from the XRD measurements.

H₂-TPR: Fig. 4 shows the H₂-TPR profiles of the Cu/AC catalysts and carbon support. The Cu/AC catalysts produce three peaks, indicating reduction in three stages, 150-300, 300-450 and 450-800 °C. The peak positions and relative contributions of the copper species of different valence states calculated from the H₂-TPR profiles are listed in Table-2.
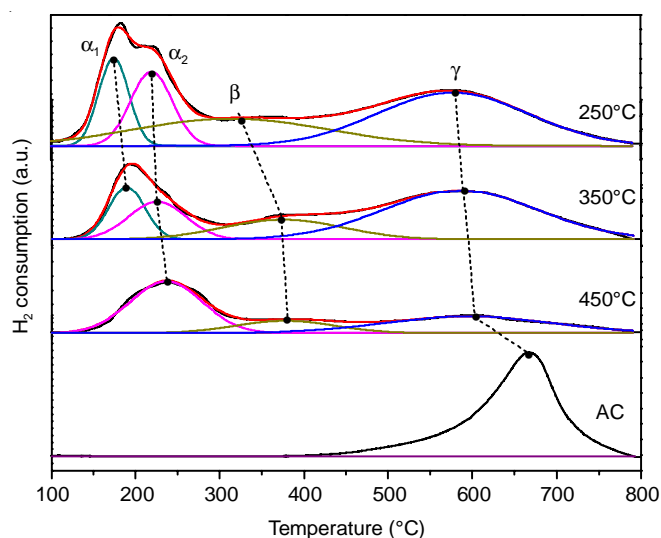
Fig. 4. H₂-TPR profiles of Cu/AC catalysts prepared at different temperatures

For the Cu/AC catalysts prepared at 250 and 350 °C, the first hydrogenation consumption peak can be deconvoluted into an α_1 peak and an α_2 peak, attributed into the reduction of well-dispersed CuO[45] and Cu^{2+}, respectively, immobilized on to the functional groups of the active carbon[46]. The second peak, labelled the β peak, is observed in the range 300 to 450 °C

TABLE-1
TEXTURAL CHARACTERISTICS OF CARBON SUPPORT AND Cu/AC CATALYSTS PREPARED AT DIFFERENT TEMPERATURES

Sample	S_{BET} [a] (m²/g)	V_p [b] (m³/g)	d_P [c] (nm)	V_{micro} [d] (m³/g)
AC	864	0.49	2.26	0.22
Cu/AC-250	582	0.34	2.31	0.16
Cu/AC-350	645	0.38	2.34	0.13
Cu/AC-450	639	0.37	2.32	0.13

[a]Specific surface area calculated from the linear part of the BET plot (P/P₀ = 0.05-0.30); [b]Pore specific volume; [c]Mean pore diameter;
[d]*t*-Plot micropore volume

TABLE 2
H$_2$-TPR QUANTITATIVE ANALYSIS RESULTS OF Cu/AC CATALYSTS PREPARED AT DIFFERENT TEMPERATURES

Temperature (°C)	Peaks			Total area	Concentrations[a]		
	α_1 Temperature (%)	α_2 Temperature (%)	β Temperature (%)		$W_{Cu}^{2+ b}$ mg (%)	$W_{Cu}^{+ c}$ mg (%)	$W_{Cu}^{0 d}$ mg (%)
250	174.5(25.3)	219.2(28.3)	313.5(47.4)	141603.4	8.8 (48.9)	8.0 (44.2)	1.2 (6.9)
350	189.8(29.7)	225.9(33.6)	374.2(36.7)	102286.0	6.2 (34.3)	3.6 (20.3)	8.2(45.4)
450	-	236.4(75.5)	377.7(24.5)	54481.6	5.5 (30.6)	1.9 (10.7)	10.6(58.7)

[a]Total copper content: 18.0 mg; [b]W_{Cu}^{2+} calculated from the area of H$_2$ consumption of peaks α_1 and α_2; [c]W_{Cu}^{+} calculated from the area of H$_2$ consumption of peak β; [d]$W_{Cu}^{0} = W_{Cu}^{Total} - W_{Cu}^{2+} - W_{Cu}^{+}$

and can be assigned to the reduction of Cu$_2$O, while the third peak (the γ peak) appears between 450 and 800 °C and corresponds to the gasification of active carbon[47], as confirmed by the blank test. For the above reasons and based on the amount of hydrogen consumption of α_1, α_2 and β peaks, the oxidation state of copper species can be quantitatively determined. The amount of Cu^0 can be obtained by subtracting the total of the Cu^{2+} and Cu$^+$ species from the total copper content.

As shown in Table-2, the amount of Cu^{2+} and Cu$^+$ species decreases, but the content of Cu^0 increases with the increase of the preparation temperature of the Cu/AC catalysts. This result can be understood because the higher valence copper species were increasingly transformed to lower valence copper species through the carbothermic reduction[48,49]. The result also indicates the presence of a certain amount of Cu^{2+} species in the Cu/AC catalysts obtained at 350 and 450 °C, although this cannot be observed in XRD measurement. It is noted that the well-dispersed CuO disappears, but the Cu^{2+} immobilized on to the functional groups increases slightly for the catalyst prepared at 450 °C. This result implies that anchored Cu^{2+} species cannot be reduced to low valence copper species *via* carbothermic reduction, but may be attributed to the super-strong interaction between Cu^{2+} and the functional groups on the support.

XPS: The XPS spectra of the Cu 2p core regions acquired from samples calcined at different temperatures are shown in Fig. 5, with appropriate curve fits. The peaks of the three catalysts were different in shape and intensity, which suggests differences of bonding type and energy of Cu species[50]. The band around 934.1 eV is characteristic of the divalent copper ion and the strong satellite structure of copper ion is observed in the XPS spectra, confirming the existence of Cu^{2+} species on the surface of all the samples. LMM Auger spectroscopic measurements performed with different samples are shown in Fig. 6. After peak fitting, two peaks are revealed in the vicinity of 914 and 917 eV, for which the values of α' are 1848 and 1851 eV, respectively. According to the literature[36], the α' values for Cu^{1+} and Cu^0 are 1849 and 1851 eV, respectively. Thus, the peaks at 913.5-914.7 eV can be assigned to the Cu$_2$O phase. The presence of peaks with large areas at 917.2-917.4 eV indicates that Cu^0 is the major copper species on the surface of the catalysts. Elemental chemical analysis in the near surface region of different Cu/AC catalysts is shown in Table-3. The concentration of metallic Cu on the surface of the catalyst gradually increases with the increase of microwave treatment temperature. The atomic ratio Cu/O/C is 1:7:31, 1:5:24 and 1:3:18 on the surface of the Cu/AC catalysts prepared at 250,
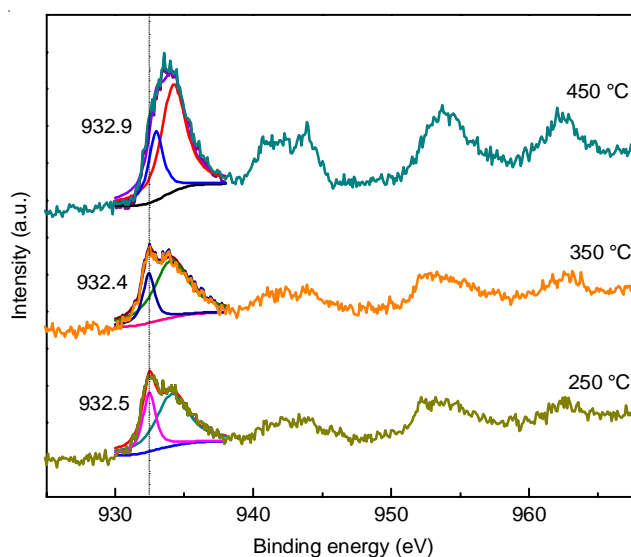
Fig. 5. Cu 2p core-level XPS spectra of Cu/AC catalysts prepared at different temperatures
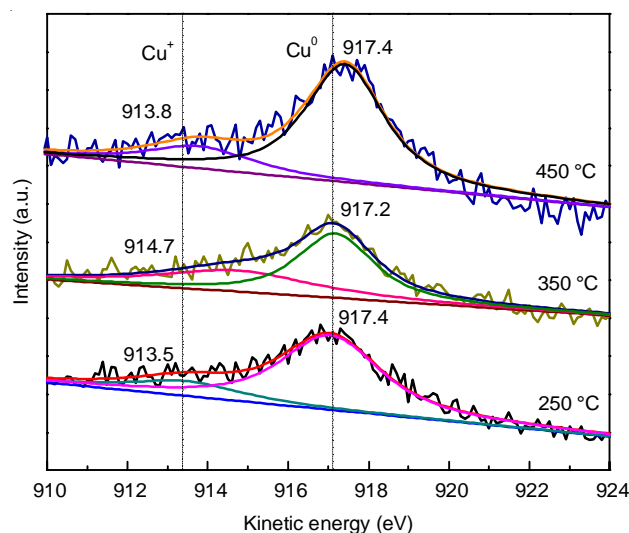
Fig. 6. Cu LMM Auger spectra of Cu/AC catalysts prepared at different temperatures

350 and 450 °C, respectively. This gives direct evidence that the Cu^{2+} species is gradually reduced to Cu^0 as the treatment temperature increases. Moreover, higher temperature also leads to enrichment of copper on the surface of the catalyst.

SEM: Fig. 7 shows SEM photographs of different Cu/AC catalysts. The size of particles on the surface of the sample obtained at 250 °C is in the range 100-200 nm. Combining this with the results of the XRD analysis, the particles should

TABLE-3
ELEMENTAL CHEMICAL ANALYSIS IN THE NEAR SURFACE REGION
OF Cu/AC CATALYSTS PREPARED AT DIFFERENT TEMPERATURES

Temperature (°C)	BE (eV)		KE (eV)		Atom concentration (%)			Cu/O/C
	Cu^{2+}	$Cu^{1+} + Cu^0$	Cu^{1+}	Cu^0	C	O	Cu	
250	934.2	932.5	913.5	917.1	80.18	17.22	2.6	1:7:31
350	934.1	932.4	914.7	917.2	80.76	15.94	3.3	1:5:24
450	934.3	932.9	913.8	917.4	80.12	15.36	4.5	1:3:18
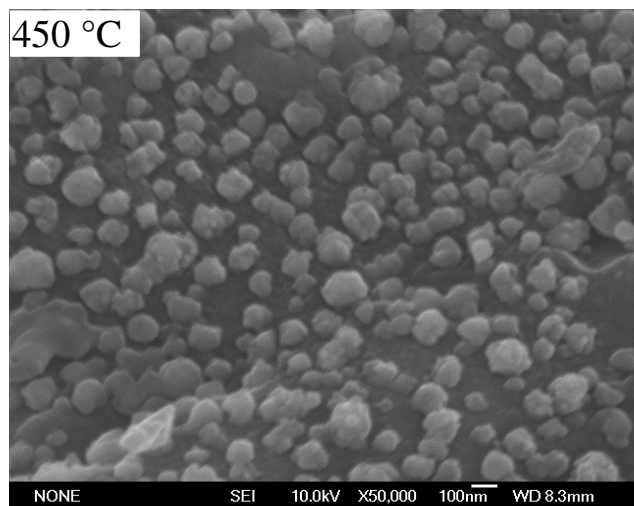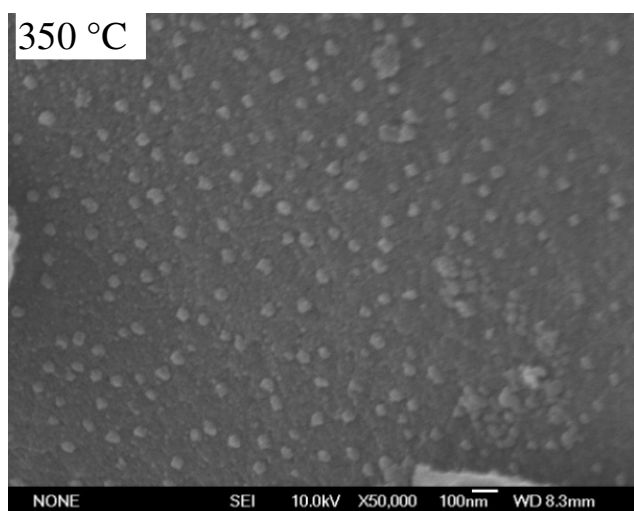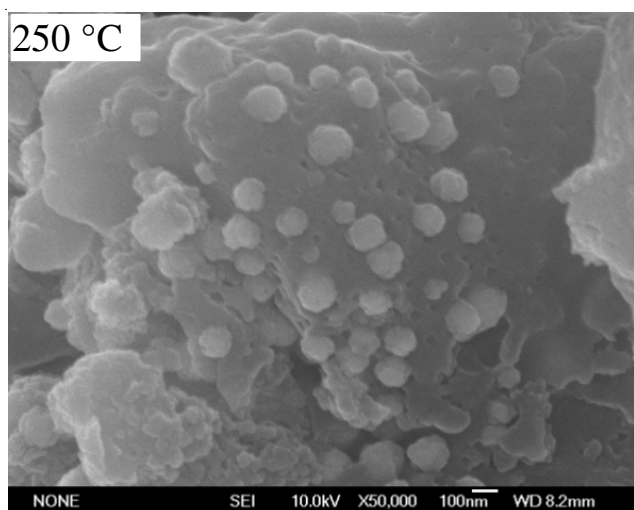
Fig. 7. SEM images of Cu/AC catalysts prepared at different temperatures

be CuO and Cu_2O. For the sample prepared at 350 °C, the particles on the catalyst surface are smaller and more uniform in size than that prepared at 250 °C and the average particle size is about 40 nm. The XRD analysis suggests that these particles are metallic copper. However, the size of the particles on the surface of the sample obtained at 450 °C is significantly larger, with some particles as much as 200 nm diameters. This is probably caused by the aggregation of Cu particles at higher temperature[29]. This observation is supported by the XRD analysis, which shows that the average particle size rises to 46.5 nm.

In conclusion, the microwave irradiation causes copper species to be reduced to uniform Cu particles at a particular temperature. The size of the Cu nanoparticles plays a crucial role in the catalytic performance of Cu/AC catalysts for the oxidative carbonylation of methanol.

Conclusion

Microwave heating of Cu/AC precursors in vacuum causes rapid decomposion of copper nitrate and further auto-reduction of copper(II) species to copper(I) oxide and Cu metal, induced by interaction with the carbon support. The heating temperature has a significant effect on the chemical form of the copper species and the catalytic performance of these Cu/AC catalysts for the oxidative carbonylation of methanol. It is found that the catalytic activity of Cu/AC is greatly dependent on the dispersion and grain size of the Cu nanoparticles. The copper species cannot be completely reduced at the low heating temperature of 250 °C and is mainly present as CuO and Cu_2O. When the heating temperature at is 350 °C, the copper species is mostly reduced to metallic copper and is in the form of uniform Cu^0 nanoparticles in the size of around 40 nm diamter. This results in the highest catalytic activity. Higher treatment temperature, up to 450 °C, results in the aggregation of Cu nanoparticles and the decrese of the catalytic activity of the Cu/AC catalyst.

REFERENCES

1. W.C. Peng, N. Zhao, F.K. Xiao, W. Wei and Y.H. Sun, *Pure Appl. Chem.*, **84**, 603 (2012).
2. M.A. Pacheco and C.L. Marshall, *Energy Fuels*, **11**, 2 (1997).
3. Y. Sato, M. Kagotani, T. Yamamoto and Y. Souma, *Appl. Catal. A*, **185**, 219 (1999).

4.   V. Raab, M. Merz and J. Sundermeyer, *J. Mol. Catal. Chem.*, **175**, 51 (2001).

5.   J.C. Hu, Y. Cao, P. Yang, J.F. Deng and K.N. Fan, *J. Mol. Catal. Chem.*, **185**, 1 (2002).

6.   W.L. Mo, H. Xiong, T. Li, X.C. Guo and G.X. Li, *J. Mol. Catal. Chem.*, **247**, 227 (2006).

7.   Y. Sato, M. Kagotani and Y. Souma, *J. Mol. Catal. Chem.*, **151**, 79 (2000).

8.   W.L. Mo, H.T. Liu, H. Xiong, M. Li and G.X. Li, *Appl. Catal. A*, **333**, 172 (2007).

9.   Y. Cao, J.F. Hu, P. Yang, W.L. Dai and K.N. Fan, *Chem. Commun.*, **7**, 908 (2003).

10. S. Csihony, L.T. Mika, G. Vlád, K. Barta, C.P. Mehnert and I.T. Horváth, *Collect. Czech. Chem. Commun.*, **72**, 1094 (2007).

11. D. Delledonne, F. Rivetti and U. Romano, *Appl. Catal. A*, **221**, 241 (2001).

12. K. Tomishige, T. Sakaihori, S.I. Sakai and K. Fujimoto, *Appl. Catal. A*, **181**, 95 (1999).

13. Y.J. Wang, X.Q. Zhao, B.G. Yuan, B.C. Zhang and J.S. Cong, *Appl. Catal. A*, **171**, 255 (1998).

14. M.S. Han, B.G. Lee, I. Suh, H.S. Kim, B.S. Ahn and S.I. Hong, *J. Mol. Catal. Chem.*, **170**, 225 (2001).

15. P. Yang, Y. Cao, J.C. Hu, W.L. Dai and K.N. Fan, *Appl. Catal. A*, **241**, 363 (2003).

16. Y.Z. Yuan, W. Cao and W.Z. Weng, *J. Catal.*, **228**, 311 (2004).

17. S.T. King, *J. Catal.*, **161**, 530 (1996).

18. Z. Li, K.C. Xie and R.C.T. Slade, *Appl. Catal. A*, **205**, 85 (2001).

19. S.A. Anderson and T.W. Root, *J. Catal.*, **217**, 396 (2003).

20. Y.H. Zhang, I.J. Drake, D.N. Briggs and A.T. Bell, *J. Catal.*, **244**, 219 (2006).

21. Y.L. Shen, Q.S. Meng, S.Y. Huang, S.P. Wang, J.L. Gong and X.B. Ma, *RSC Adv.*, **2**, 7109 (2012).

22. Y.H. Zhang and A.T. Bell, *J. Catal.*, **255**, 153 (2008).

23. X.B. Zheng and A.T. Bell, *J. Phys. Chem. C*, **112**, 5043 (2008).

24. M. Richter, M.J.G. Fait, R. Eckelt, M. Schneider, J. Radnik, D. Heidemann and R. Fricke, *J. Catal.*, **245**, 11 (2007).

25. M. Richter, M.J.G. Fait, R. Eckelt, E. Schreier, M. Schneider, M.-M. Pohl and R. Fricke, *Appl. Catal. B*, **73**, 269 (2007).

26. S.T. King, *Catal. Today*, **33**, 173 (1997).

27. Y.J. Wang, R.X. Zhang, X.Q. Zhao and S.F. Wang, *J. Nat. Gas Chem.*, **9**, 205 (2000).

28. R.Y. Wang and H.Y. Zhong Li, *Chin. J. Catal.*, **31**, 851 (2010).

29. J. Ren, C.J. Guo, L.L. Yang and Z. Li, *Chin. J. Catal.*, **34**, 1734 (2013).

30. J. Ren, W. Wang, D.L. Wang, Z.J. Zuo, J.Y. Lin and Z. Li, *Appl. Catal. A*, **472**, 47 (2014).

31. B.S. Zhang, X.J. Ni, W. Zhang, L.D. Shao, Q. Zhang, F. Girgsdies, C.H. Liang, R. Schlogl and D.S. Su, *Chem. Commun.*, **47**, 10716 (2011).

32. M. Baghbanzadeh, L. Carbone, P.D. Cozzoli and C.O. Kappe, *Angew. Chem. Int. Ed.*, **50**, 11312 (2011).

33. H.E. Cross, G. Parkes and D.R. Brown, *Appl. Catal. A*, **429-430**, 24 (2012).

34. C. Antonetti, M. Oubenali, A.M. Raspolli Galletti, P. Serp and G. Vannucci, *Appl. Catal. A*, **421-422**, 99 (2012).

35. Z. Li, S.W. Yan and H. Fan, *Fuel*, **106**, 178 (2013).

36. J. Ren, S.S. Liu, Z. Li, X.L. Lu and K.C. Xie, *Appl. Catal. A*, **366**, 93 (2009).

37. S.G. Deng and Y.S. Lin, *Chem. Eng. Sci.*, **52**, 1563 (1997).

38. J. Rao, B. Vaidhyanathan, M. Ganguli and P.A. Ramakrishnan, *Chem. Mater.*, **11**, 882 (1999).

39. K.H. Chuang, C.Y. Lu, M.Y. Wey and Y.N. Huang, *Appl. Catal. A*, **397**, 234 (2011).

40. L.L. Bo, Y.B. Zhang, X. Quan and B. Zhao, *J. Hazard. Mater.*, **153**, 1201 (2008).

41. Z. Zhu, G.Q.M. Lu, Y. Zhuang and D. Shen, *Energy Fuels*, **13**, 763 (1999).

42. Z.P. Zhu, Z.Y. Liu, S.J. Liu, H.X. Niu, T.D. Hu, T. Liu and Y.N. Xie, *Appl. Catal. B*, **26**, 25 (2000).

43. J. Ren, S.S. Liu, Z. Li and K.C. Xie, *Catal. Commun.*, **12**, 357 (2011).

44. S.M. Sajjadi, M. Haghighi, A.A. Eslami and F. Rahmani, *J. Sol-Gel Sci. Technol.*, **67**, 601 (2013).

45. B. Zhang, S.G. Hui, S.H. Zhang, Y. Ji, W. Li and D.Y. Fang, *J. Nat. Gas Chem.*, **21**, 563 (2012).

46. J.L. Figueiredo, *J. Mater. Chem. A*, **1**, 9351 (2013).

47. J. Bian, M. Xiao, S.J. Wang, Y.X. Lu and Y.Z. Meng, *Catal. Commun.*, **10**, 1142 (2009).

48. M. Samouhos, R. Hutcheon and I. Paspaliaris, *Miner. Eng.*, **24**, 903 (2011).

49. D. Vennerberg, R. Quirino and M.R. Kessler, *Adv. Eng. Mater.*, **15**, 366 (2013).

50. J.K. Nam, M.J. Choi, D.H. Cho, J.K. Suh and S.B. Kim, *J. Mol. Catal. Chem.*, **370**, 7 (2013).